Monod, J., Wyman, J., and Changeux, J. P. (1965), *J. Mol. Biol. 12*, 88.
Pearlmutter, A. F., and Stuehr, J. (1968), *J. Amer. Chem. Soc. 90*, 858.
Pörschke, D., and Eigen, M. (1971), *J. Mol. Biol. 62*, 361.
Reeves, R. H., Cantor, C. R., and Chambers, R. W. (1970), *Biochemistry 9*, 3993.
Rialdi, G., Levy, J., and Biltonen, R. (1972), *Biochemistry 11*, 2472.
Robison, B., and Zimmerman, T. P. (1971a), *J. Biol. Chem. 246*, 110.
Robison, B., and Zimmerman, T. P. (1971b), *J. Biol. Chem. 246*, 4664.
Rossi-Fanelli, A., Antonini, E., and Caputo, A. (1964), *Advan. Protein Chem. 19*, 74.
Rossotti, F. J. C., and Rossotti, H. (1961), The Determination of Stability Constants, New York, N. Y., McGraw-Hill.
Saneyoshi, M., Harada, F., and Nishimura, S. (1969), *Biochim. Biophys. Acta 190*, 264.
Schofield, P., Hoffman, B. M., and Rich, A. (1970), *Biochemistry 9*, 2525.
Schreier, A. A. (1973), Ph.D. Thesis, M.I.T.
Schreier, A. A., and Schimmel, P. R. (1972), *Biochemistry 11*, 1582.
Schreier, A. A., and Schimmel, P. R. (1974), *J. Mol. Biol.* (in press).
Takahashi, K. (1961), *J. Biochem. (Tokyo) 49*, 1.
Tao, T., Nelson, J. H., and Cantor, C. R. (1970), *Biochemistry 9*, 3514.
Ward, D. C., Reich, E., and Stryer, L. (1969), *J. Biol. Chem. 244*, 1228.
Willick, G. E., and Kay, C. M. (1971), *Biochemistry 10*, 2216.
Yang, S. K., Söll, D. G., and Crothers, D. M. (1972), *Biochemistry 11*, 2311.
Yarus, M., and Barrell, B. G. (1971), *Biochem. Biophys. Res. Commun. 43*, 729.
Yarus, M., and Berg, P. (1969), *J. Mol. Biol. 42*, 171.
Yarus, M., and Rashbaum, S. (1972), *Biochemistry 11*, 2043.

Effects of Abnormal Base Ionizations on Mg^{2+} Binding to Transfer Ribonucleic Acid as Studied by a Fluorescent Probe†

Dennis C. Lynch‡ and Paul R. Schimmel*

ABSTRACT: The naphthoxyl probe attached to the 3′-end of isoleucyl-$tRNA^{Ile}$ (see Lynch, D. C., and Schimmel, P. R. (1974), *Biochemistry 13*, 1841) has been used to study the pH dependence of Mg^{2+} binding at "cooperative" sites. The apparent Mg^{2+} affinity is strongly pH dependent; *e.g.*, it is *ca.* tenfold and 100-fold weaker at pH 6 and pH 4.7, respectively, than at pH 7.5. This effect is due to abnormally high base p*K*'s in the "aberrant" structure(s) formed in low salt, Mg^{2+}-free solutions. The emission of the probe is sensitive to the ionization of one of these sites, probably a cytidylic acid moiety near the 3′-end. Addition of sufficient Mg^{2+} sharply lowers the abnormal p*K*'s to more typical values. The kinetics of Mg^{2+} addition at pH 6 appears to follow essentially the same mechanism as at pH 7.5—two slow unimolecular changes coupled to rapid Mg^{2+} binding steps. However, the Mg^{2+}-induced structural changes are slower, have somewhat higher activation energies, and are thermodynamically less favored at pH 6. These effects apparently arise from the greater stability of aberrant form(s) brought about by base protonations, and they largely account for the weaker apparent binding of Mg^{2+} observed by fluorescence at pH 6 as opposed to pH 7.5. Ultraviolet absorption data corroborate many of the findings. Preliminary results with $tRNA^{Ala}$ (*Escherichia coli*) labeled with the probe are similar to those obtained with $tRNA^{Ile}$, thus suggesting that the results obtained may be rather general.

In the preceding paper (Lynch and Schimmel, 1974), it was shown that the fluorescence emission of a naphthoxyl group attached to the 3′-end of $tRNA^{Ile}$ is sensitive to the binding of Mg^{2+} to "interacting" or "cooperative" sites on the nucleic acid. Two slow unimolecular structural changes occur as Mg^{2+} is bound to these sites; these changes have large activation energies and are probably due to the breakdown of aberrant structures formed in the absence of Mg^{2+} (see Cole *et al.*, 1972). Since the structural changes induced by Mg^{2+} binding are thermodynamically favorable, they serve to increase the apparent strength of binding of Mg^{2+}. This accounts for the high affinity of Mg^{2+} binding to these sites.

At pH 6 we were surprised to learn that the binding of Mg^{2+} observed by fluorescence is significantly weaker than that observed at pH 7.5 (Lynch and Schimmel, 1974), even though there are no obvious base or phosphodiester ionizations in this pH range. The results presented below demonstrate that abnormal p*K*'s (on bases) are present on tRNA and that protonation of these sites leads to an increased stabilization of the "aberrant" structure(s) formed in low salt. Addition of Mg^{2+} sharply lowers the abnormal p*K*'s and encourages proper folding of the tRNA, although the folding process itself is somewhat slower and goes with higher activation energies at the more acid pH (pH 6) than at pH 7.5. The decreased thermodynamic preference for the Mg^{2+}-induced

† From the Departments of Biology and Chemistry, Massachusetts Institute of Technology, Cambridge, Massachusetts 02139. *Received October 23, 1973.* This work was supported by grant no. GM-15539 from the National Institutes of Health. Material for this manuscript was taken from the Ph.D. thesis of Dennis C. Lynch (Massachusetts Institute of Technology, 1973).

‡ Present address: Division of Biology, California Institute of Technology, Pasadena, Calif. 91109. Predoctoral Fellow of the National Institutes of Health, 1970–1973.

structural changes at pH 6 largely accounts for the weaker apparent binding at this pH as opposed to pH 7.5.

Materials and Methods

Many of the details of the preparation of materials, treatment of data, instrumentation, and etc., are given in the preceding paper (Lynch and Schimmel, 1974). Additional details pertinent to the present paper are given below.

Derivatized isoleucyl-tRNA^{Ile} in which the 5′-phosphate is removed was prepared by incubating IV[1] for 1 hr at 53° in 0.05 M Tris–0.1 mM $MgCl_2$ (pH 7.5) with *ca.* 1 μg of bacterial alkaline phosphatase (Worthington BAPF grade) per nmole of tRNA. These conditions, which are slightly milder than usual phosphatase conditions, were chosen in order to minimize hydrolysis of the label. Under these conditions, <15% of the label was lost. Phosphatase was removed *via* phenol extraction and an aliquot of the tRNA was digested for 5 hr at 37° in 0.01 M $(NH_4)_2CO_3$ (pH 8) with *ca.* 2 μg of RNase A (Worthington) per nmole of tRNA. This digest and a control not treated with phosphatase were applied to separate 20 × 20 cm cellulose thin-layer plates (E. Merck) and chromatographed in two dimensions (first dimension: 1-propanol–concentrated ammonia–water, 55:10:35 by volume; second dimension: isobutyric acid–concentrated ammonia–water, 66:1:33 by volume; U. L. RajBhandary and M. Simsek, personal communication; see also Saneyoshi *et al.* (1969)). The resultant patterns were examined under an ultraviolet lamp and found to be identical except that a slow moving oligonucleotide spot present in the control was absent in the phosphatase treated material. We attribute the missing spot to the 5′-terminal fragment pApGpGpCp which would be converted to ApGpGpCp by successful phosphatase removal of the tRNA 5′-phosphate. As there is another expected RNase A fragment of this identity (see Yarus and Barrell, 1971), a new spot is not expected in the phosphate treated pattern. Thus the chromatograms provide fair, although not rigorous, evidence that the 5′-phosphate was removed.

Polarization of fluorescence was measured with a Farrand Optical Company Mark I spectrofluorometer employing films supplied by the manufacturer. The measured values were corrected for apparent polarization introduced by the monochromator by the method of Azumi and McGlynn (1962; see also, Chen and Bowman (1965)). Fluorescence stopped-flow experiments were performed with a Durrum-Gibson stopped-flow equipped with a 75-W xenon lamp (General Electric). The apparatus has a dead time of less than 5 msec. (We gratefully acknowledge the use of this instrument at the Peter Bent Brigham Hospital, in the laboratory of Dr. B. Vallee. The helpful assistance of Dr. D. Auld is also acknowledged.) Fluorescence lifetimes were measured with the single photon counting system designed by Ortec in the laboratory of Dr. Renata Cathou at Tufts University Medical Center (see Lynch (1973), for additional details). The permission granted by Dr. Cathou to use the instrument, and the extensive help given by Dr. James Bunting are gratefully acknowledged.

The pH measurements made in fluorescence pH titrations were performed on thermostated samples not containing tRNA. The pH was measured directly with a Radiometer pH meter equipped with a GK2021C electrode; titrations were generally reproducible to within ±0.03 pH unit. The samples containing tRNA which were used for optical measurements were then titrated in the same way, but without directly measuring the pH. This procedure proved to be more efficient and also necessary because of fluorescence contamination introduced by the electrode. Fluorescence and uv titration were on occasion checked for reversibility. These titrations were generally found to be reversible over most of the pH range studied. Difficulty was sometimes encountered at acid pH values which promote incipient precipitation of tRNA.

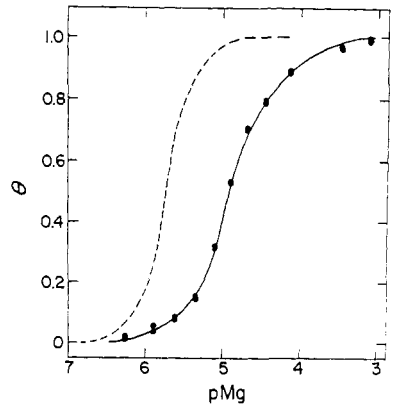

FIGURE 1: Relative change in fluorescence (θ) *vs.* pMg. Solid curve with points applies to data at pH 6.0, 10 mM Na^+, 1 mM EDTA, 20 mM cacodylate, and Cl^- counterion. Dashed curve applies to data at pH 7.5, 10 mM Na^+.

EDTA was used to buffer Mg^{2+} concentrations as was done in the preceding study (Lynch and Schimmel, 1974). The stability constant of the Mg^{2+}–EDTA complex increases with increasing pH (see Laitinen, 1960). Fortunately, this pH dependence is in the same direction as the pH dependence of Mg^{2+} binding to tRNA. This allowed the use of EDTA at several different pH values and concentrations to buffer Mg^{2+} in different concentration ranges.

Organic liquids used in fluorescence experiments were distilled when they contained obvious optical impurities.

Results and Treatment of Data

pH Dependence of Mg^{2+} Binding. Fluorescence Mg^{2+} titration of the derivatized tRNA at pH 6 gave strikingly different results than those obtained at pH 7.5. Figure 1 gives a plot of the fractional change in fluorescence θ *vs.* pMg at pH 6. For comparison, the results obtained at pH 7.5 are shown by a dashed line. It is clear from this figure that the Mg^{2+} binding observed by fluorescence is substantially weaker and less cooperative at pH 6.0 than at pH 7.5. This result is somewhat surprising since *a priori* it is not immediately apparent that there are any groups on tRNA which ionize in this region, except for the 5′-terminal phosphate. Any involvement of this group was eliminated, however, by the finding that the Mg^{2+} binding followed by fluorescence was not altered by apparent removal of this group with bacterial alkaline phosphatase.

The pH dependence of the Mg^{2+} binding was further pursued by performing fluorescence titrations at pH 4.7. The data obtained at the various pH values are tabulated in Table I in terms of the apparent dissociation constant K_{app} and the empirical Hill coefficient n. These parameters were obtained as described in the preceding paper (Lynch and Schimmel, 1974). In addition, some data on Na^+ titrations are given also.

These data show a remarkable pH dependence of the Mg^{2+} affinity for tRNA. The affinity changes somewhat less than an

[1] Abbreviation used is: A_λ, the absorbance at wavelength λ of a solution in a 1-cm path-length cell. Structures I–IV are defined in Lynch and Schimmel (1974).

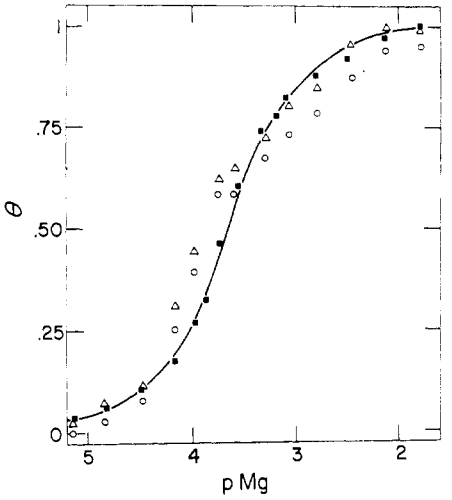

FIGURE 2: Plot of θ *vs.* pMg at pH 4 7, 25° with a buffer of 70 mM Na^+, 0.1 M acetate, 10 mM EDTA, and Cl^- counterion: (■) θ for fluorescence; (○) θ for A_{260}; (Δ) θ for A_{280}. Curve is drawn for fluorescence points.

TABLE I: pH-Dependence of Mg^{2+} and Na^+ Binding at 25°.

pH	[Na^+] (mM)	pK_{app}	n
	Mg^{2+} Titrations		
7.5[a]	10	5.73	2.30
	37	5.79	1.52
6.0	10[b]	4.84	1.26
	45[c]	4.74	0.99
4.7	10[d]	3.9[f]	
	70[e]	3.66	1.14
	100[e]	3.70	1.06
	Na^+ Titrations		
7.5		1.52	2.10
6.0		1.33	1.8
4.7		0.82	1.76

[a] See Lynch and Schimmel (1974) for details. [b] 20 mM cacodylate, 1 mM EDTA, and Cl^- counterion. [c] 100 mM cacodylate, 1 mM EDTA, and Cl^- counterion. [d] 10 mM acetate, 1 mM EDTA, and Cl^- counterion. [e] 100 mM acetate, 10 mM EDTA, and Cl^- counterion. [f] Curve is very unsymmetric.

order of magnitude for each pH unit. Furthermore, the cooperativity is most pronounced at pH 7.5 and is significantly less at the other pH values. The binding of Na^+ is also dependent on pH, although less markedly than Mg^{2+}. However, at all pH values Na^+ exerts relatively little influence on the apparent Mg^{2+} dissociation constant although it does depress the cooperativity.

At this point it is worth asking whether the remarkable pH effects are due to general effects of hydrogen ion on tRNA structure or if they might rather be due to a highly localized phenomenon sensed by the fluorescence probe. To answer this question, the small uv absorbance changes accompanying Mg^{2+} binding were also studied at each of the pH values. Figure 2 gives results obtained at pH 4.7 where θ (=fractional change in absorbance or fluorescence) *vs.* pMg is given. The points for fluorescence (■) and absorbance (A_{260} = ○; A_{280} = Δ) fall about the same curve. An approximately similar correlation was found at pH 6.0. This indicates that the emission and absorbance changes occur in the same general region and that the pH induced effects are doubtless associated with the overall tRNA structure and not just a localized area.

pH Dependence of Fluorescence. The magnitudes of the emission changes associated with the Mg^{2+} binding discussed above are dependent on the pH. This indicates, of course, that the probe's emission is sensitive to hydrogen ion as well as metal ions. This is clearly seen in Figure 3a where the relative fluorescence at 350 nm is plotted *vs.* pH for two different conditions. The upper curve was obtained in 10 mM Mg^{2+}; the lower curve was obtained in Mg^{2+}-free solutions containing 10 mM Na^+. It is clear that under both conditions the emission is strongly pH dependent and appears to follow a simple titration curve. The magnitude of the emission changes and the apparent midpoints of the titration curves are very different, however. In both cases, the high pH plateau is achieved by pH 7.5, so that the Mg^{2+} titrations discussed in

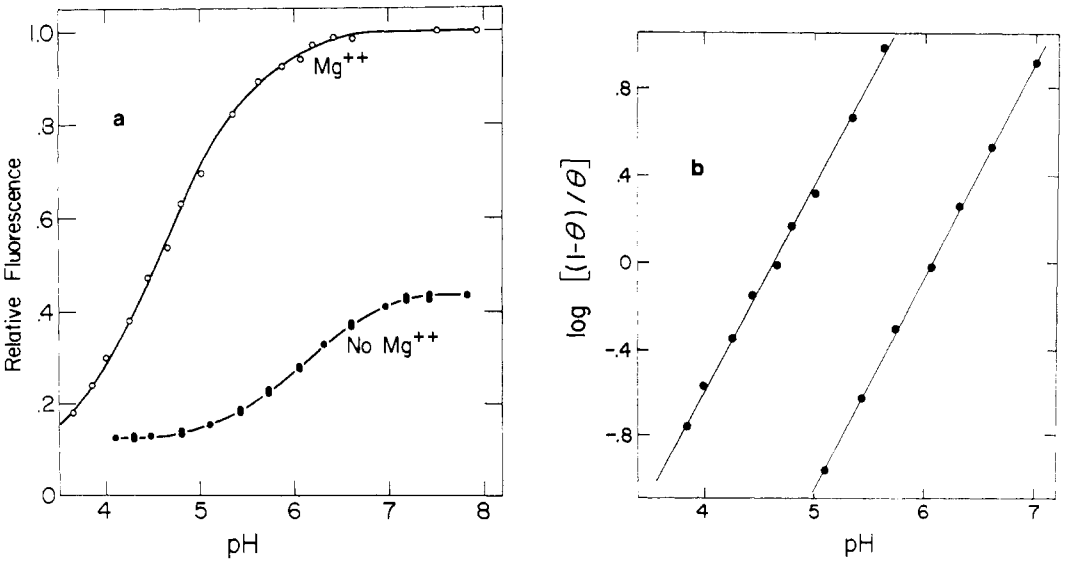

FIGURE 3: (a) Relative fluorescence emission *vs.* pH. The upper curve was obtained in 10 mM Mg^{2+} and the lower curve in 10 mM Na^+. Details of experimental procedure are given in Table II. Points on the upper curve are averages of three experiments; those on the lower curve are from two experiments with scatter as shown (where there is only one point, observed values coincided). (b) Plot of log $(1 - \theta)/\theta$ *vs.* pH for data derived from curves in Figure 3a.

TABLE II: Fluorescence pH Titrations of Labeled tRNA at 25°.

Cation (concn, mM)	Method	pK_H	n	Quenching[e]
Na^+ (10)	*a*	6.04 ± 0.03	1.01 ± 0.02	0.30
Na^+ (0.55 M)	*b*	4.57 ± 0.06	0.95 ± 0.04	0.11
Mg^{2+} (10)	*c*	4.63 ± 0.05	0.99 ± 0.04	0.12
Mn^{2+} (10)	*d*	4.64 ± 0.04	0.95 ± 0.03	0.19
Spermidine^{3+} (1)	*b*	4.74 ± 0.05	1.01 ± 0.03	0.16

[a] Buffer contained 3 mM EDTA, 10 mM Na^+, and Cl^- counterion. Titration was from high pH to low pH with 0.1 and 1.0 M acetic acid. [b] Buffer contained 5 mM EDTA, 5 mM acetate, 10 mM NaCl, and 10 mM cacodylate, titrated from low pH to high pH with 0.1 M NaOH. [c] Buffer contained 10 mM cacodylate, 5 mM acetate, and 10 mM NaCl, titrated from low pH to high pH with 0.1 M NaOH. [d] Buffer contained 10 mM cacodylate and 10 mM NaCl; titration with 0.1 and 1.0 M acetic acid was from high pH to low pH. [e] Ratio of emission at low pH plateau to that at high pH plateau.

the preceding paper (Lynch and Schimmel, 1974) monitor the transition from one plateau to the other. There is clearly a low pH plateau on the low salt curve, and the high Mg^{2+} curve is apparently heading toward one. (Experiments below pH 3.5 could not be carried out because the tRNA precipitates at acid pH.)

The curves in Figure 3a were replotted as log $[(1 - \theta)/\theta]$ *versus* pH according to the simple ligand binding scheme of the preceding paper (Lynch and Schimmel, 1974). The results are given in Figure 3b which shows that the data are very linear over the range $0.1 < \theta < 0.9$ and conform well to a single pK. Similar titrations were performed in the presence of large amounts of Mn^{2+} and spermidine as well. Table II summarizes the hydrogen ion pK_H and n values obtained. In every instance the data fit that for a single site with the cation stabilized form of the tRNA having its pK_H shifted about 1.3–1.4 units below that of the low salt form. The fact that the data fit that for a single pK under a variety of conditions indicates that the probe is probably monitoring just one ionization site on the tRNA, although the changes in Mg^{2+} affinity with pH may be brought about by ionizations at several sites.

What is the identity of these ionization sites? Although the pH dependence of tRNA structure has previously not been well studied, DNA and several synthetic polyribonucleotide systems have been well characterized with respect to pH dependent behavior. For example, strongly salt dependent pK_H values have been observed for protonations of the bases in DNA; in general, the lower the salt concentration, the higher the pK_H. Values between $pK_H = 4.0$ and 6.1 for deoxycytidylic acid residues, and between $pK_H = 3.5$ and 5.4 for deoxyadenylic acid residues in DNA have been reported (Cavalieri and Stone, 1955; Jordan, *et al.*, 1956; Cox and Peacocke, 1957; see Jordan, 1960, for an extensive review), whereas the monomers have approximately salt independent pK_H values of 4.2 and 3.6, respectively (Cavalieri and Stone, 1955). Protonation of the adenine bases in poly(A) leads to the formation of a double helix in which each adenine forms three hydrogen bonds (Rich *et al.*, 1961). The protonation occurs about $pK_H = 5.9$ in 0.1 M K^+ and is "severely depressed" by 2 mM Ca^{2+} (Beers and Steiner, 1957; Steiner and Beers, 1959). Poly(C) can form a double helical, triple hydrogen bonded structure which exhibits pK_H's in solution of 5.7 and 3.0,

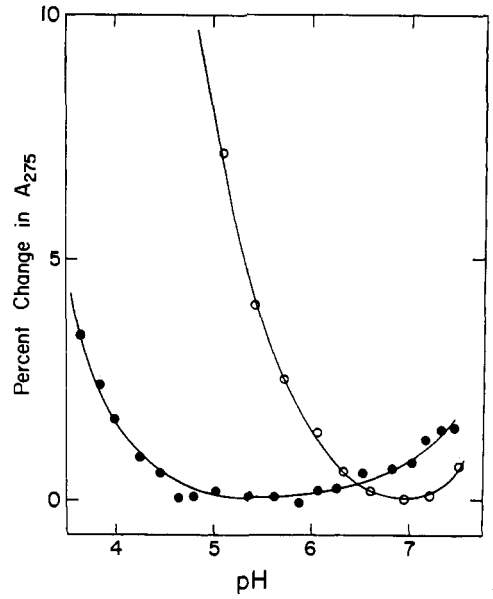

FIGURE 4: Per cent change in A_{275} *vs.* pH at 25°. Buffers are as for corresponding experiments in Figure 3a: (●) data obtained in the presence of 10 mM Mg^{2+}; (○) data obtained in the presence of 10 mM Na^+, no Mg^{2+}. Details as for corresponding fluorescence titrations given in Table II.

compared with a pK_H of 4.2 for cytidylic acid (Langridge and Rich, 1963; Hartman and Rich, 1965). Each protonation corresponds to the addition of one proton per base pair. The abnormal pK_H values are interpreted as being a result of the first proton binding more readily ($pK_H = 5.7$) to allow formation of a particular hydrogen bond and subsequent helix formation, and the second proton binding weakly ($pK_H = 3.0$) because its presence destroys the helix.

In each of these examples, protonation at the elevated pK_H leads to the formation of additional structure in the polynucleotide. Therefore, it is plausible that protonation of specific groups on tRNA leads to additional structure, although not necessarily the same kinds of structures observed in cases mentioned above.

The ultraviolet absorption of unacylated $tRNA^{Ile}$ was studied as a function of pH in order to assess further the pH dependent structural effects. Since A and C residues are likely to cause a pH effect, particular attention was directed to measurements at 275 nm where the protonation of C has its largest change (protonation of A causes almost no change in its spectrum (Cavalieri and Stone, 1955; Hartman and Rich, 1965)). Figure 4 shows the pH titration monitored at 275 nm of unacylated $tRNA^{Ile}$ in 10 mM Mg^{2+} and in 10 mM Na^+. The changes are rather small. The data definitely show, however, that the uv absorption at 275 nm is pH dependent. The titration curves do not appear to have a simple structure, presumably because the uv absorption change is made up of the overlapping contributions of many bases. However, the relative positions of the titration curves are markedly shifted by Mg^{2+} in a way which qualitatively resembles the effects followed by emission changes (Figure 3a). It seems likely from the uv absorption data that more than one C is being protonated in the region where the probe shows a pH dependence of its fluorescence. Although no specific data were obtained, it is reasonable to suspect that one or more A residues is also protonated in this region.

As mentioned above, the fluorescence data suggest that the probe is sensitive to only one of these "abnormal" ionizations. To check on the effects of nearby ionizations on the naph-

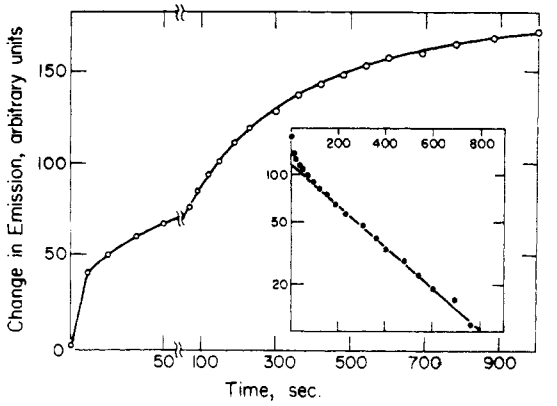

FIGURE 5: Change in fluorescence emission intensity with time following the addition of Mg^{2+} at pH 6.0, 25° with a buffer of 20 mM cacodylate, 1 mM EDTA, 10 mM Na^+, and Cl^- counterion. Addition of Mg^{2+} resulted in a final free Mg^{2+} concentration of 6.3×10^{-5} M. The inset gives a semilogarithmic plot of the final signal minus the current signal *vs.* time.

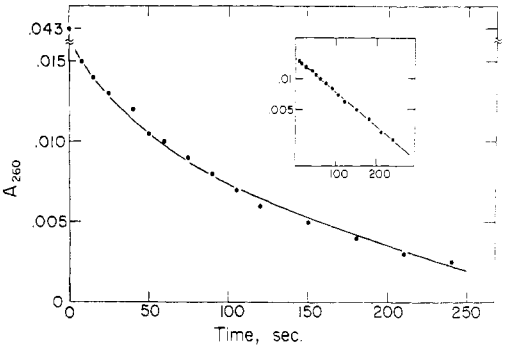

FIGURE 6: Change in A_{260} with time following the addition of Mg^{2+}, pH 6.0, 25° with buffer as in Figure 5. Inset is ΔA_{260} on logarithmic scale. Addition resulted in a free $[Mg^{2+}] = 9.5 \times 10^{-5}$ M.

thoxyl group's fluorescence, the pH dependence of the emission of the parent compound I and the fragments II and III was studied. All of these molecules display pH-dependent emission changes which follow a single pK_H. These titrations were different in two major respects from that of the label attached to intact tRNA, however. First, the quenching observed as the pH is lowered is significantly less than that found with intact tRNA (Lynch, 1973). Second, the titrations of I, II, and III are *independent of* Mg^{2+} which markedly contrasts with the results shown in Figure 3a for IV. In the case of I a $pK_H = 2.4$ was found. The pK_H apparently corresponds to ionization of the carboxyl group (phenoxyacetic acid has a carboxyl $pK_H = 3.15$ (Hayes and Branch, 1943)). The observed fluorescence level and pH dependence of I in the pH 3.5–8 range are not changed if unmodified tRNA is added to the solution in fourfold greater concentration than is normally used in titrations of IV. This indicates that the fluorescence of the naphthoxyl moiety is not greatly influenced by the tRNA if they are not covalently bonded together.

A $pK_H = 3.8$ was observed for II. This pK_H closely corresponds to a pK_H of adenosine (Alberty *et al.*, 1951). This result suggests that the fluorescence of the naphthoxyl group is able to monitor protonations in its vicinity.

In the case of III, almost all of the signal change conforms to a smooth titration curve centered at pH 4.8; there was slight (<5% of the initial signal) additional quenching below pH 3.5 which was not studied. The pK_H value of 4.8 is about 1.2 units above that for the adenine base of AMP (Alberty, *et al.*, 1951) and 0.6 unit above that for the cytosine base of CMP (Hartman and Rich, 1965). Thus, it seems likely that a C rather than an A is responsible for the changes in fluorescence seen in III. If a cytidine(s) is responsible, the results indicate that the probe is sensitive to a protonation at a nonadjacent base in the primary structure.

The salt independent $pK_H = 4.8$ for III is very close to that observed in the high salt form of IV, which raises the possibility that the same group is causing the fluorescence changes in III and in IV. Of the four C residues in III, the two closest to the probe are not base paired in the tRNA cloverleaf structure. Either of them are plausible candidates for the locus of the protonation causing the fluorescence changes in IV.

Kinetic Studies at pH 6. The kinetic studies of Mg^{2+} binding reported in the preceding paper (Lynch and Schimmel, 1974) were done at pH 7.5 where the emission exhibits no pH dependence. To investigate further the mechanism of coupling of the "abnormal" hydorgen ion equilibria with the cooperative binding of Mg^{2+}, kinetic studies were carried out at pH 6. At this pH (in 10 mM Na^+), the cooperativity index n is reduced about twofold and the apparent Mg^{2+} dissociation constant almost tenfold from the values observed at pH 7.5 (see Table I).

Figure 5 gives a plot of the time course of the fluorescence increase ΔF following Mg^{2+} addition at 25°. The kinetics clearly appear to involve at least three phases—a rapid jump followed by two slower phases. The inset in the figure gives log ΔF *vs.* time. When the longer time portion of the semilogarithmic plot is subtracted from the total signal, the early time portion also yields a straight line when the data are replotted. However, unlike the case at pH 7.5, when the straight lines are extrapolated back to zero time, they do *not* account for all of the intensity change that occurs. This is a consequence of the rapid initial jump in fluorescence.

Similar rates for Mg^{2+} induced optical density changes were observed by monitoring the absorbance of unacylated $tRNA^{Ile}$ at 260 nm (see Figure 6). Although the changes are quite small (~5%), the time course may be resolved into two straight line sections on a semilogarithmic plot with the same rates as observed in the fluorescence experiments. The changes in optical density are observed with derivatized tRNA as well as the unacylated species. Since the uv changes are in general agreement with the fluorescence results, and since the same rates are observed for unacylated as well as derivatized $tRNA^{Ile}$, it is concluded that at pH 6, as at pH 7.5, the probe is monitoring, but not influencing, a general tRNA conformational change.

The linearity of the semilogarithmic plots indicates that first-order, or pseudo-first-order, kinetic processes are causing the fluorescence changes. However, since the two observed processes do not account for all of the signal change, one (or more) additional rapid process is necessary to describe the observed overall change ΔF to give

$$\Delta F = \Delta F' + A_1 e^{-\lambda_1 t} + A_2 e^{-\lambda_2 t} \quad (1)$$

where $\lambda_1 > \lambda_2$, $\Delta F'$ is the rapid initial change in fluorescence that occurs on Mg^{2+} addition, A_1 and A_2 are amplitude parameters, and λ_1 and λ_2 are time constants. The parameters λ_1 and λ_2 are plotted as functions of the Mg^{2+} concentration (at 10 mM Na^+) in Figures 7a and b. Each exhibits a hyperbolic Mg^{2+} dependence. The lines in the figures are theoretical curves which are derived below. This behavior of λ_1 and λ_2 implies that these two rate processes represent slow unimolecular changes coupled to rapid bimolecular step(s). Thus, the slower time portions of the kinetics are qualitatively similar at pH 6 and pH 7.5.

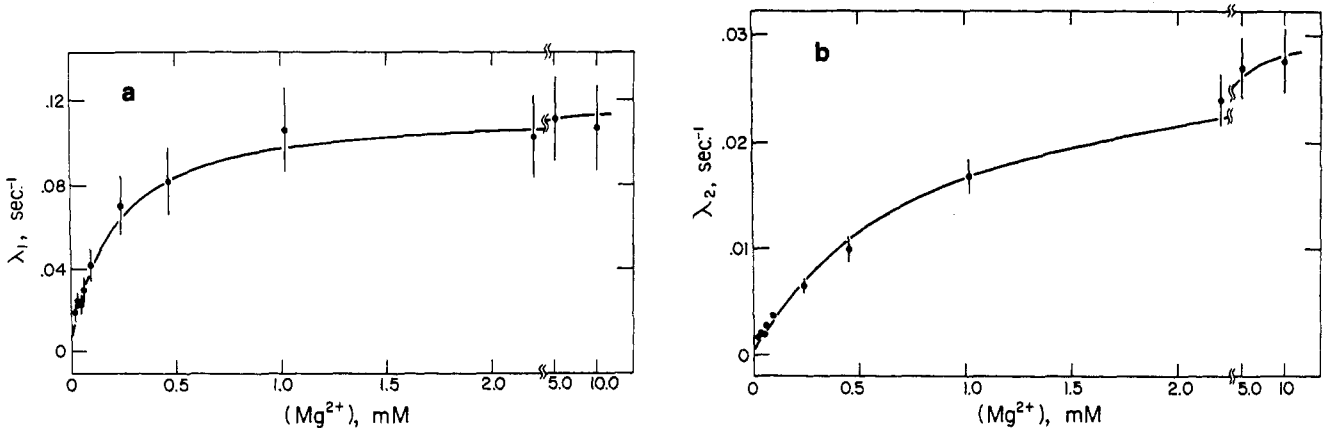

FIGURE 7: (a) Plot of λ_1 *vs.* [Mg^{2+}] at pH 6.0, 25°. Points are averages of several experiments, the error bars are ±20%. All experiments were done in 10 mM Na^+, 20 mM cacodylate, 1 mM EDTA, and Cl^- counterion. The line is a theoretical curve calculated as described in the text with the parameters listed in Table III. (b) Plot of λ_2 *vs.* [Mg^{2+}]; the error bars are ±10%. See legend to Figure 7a for further details.

In order to resolve the rate of the initial jump $\Delta F'$, fluorescence stopped-flow experiments were performed. It was observed that for Mg^{2+} additions giving Mg^{2+} concentrations of 10^{-3} and 10^{-4} M, the portion of the signal change corresponding to $\Delta F'$ was completely over within the dead time of the instrument ($\sim 5 \times 10^{-3}$ sec). This indicates that any bimolecular Mg^{2+} binding step(s) involved in generating $\Delta F'$ must have a rate constant(s) greater than *ca.* 2×10^6 M^{-1} sec^{-1}. This is of the order seen for reaction between Mg^{2+} and ADP in a temperature-jump study (see Eigen and Hammes, 1960).

Despite the inability to measure a rate for $\Delta F'$, valuable information may be obtained from the Mg^{2+} dependence of its magnitude. Figure 8a gives a plot of θ_J *vs.* pMg where θ_J is the fractional change (of its maximal change) of $\Delta F'$, and Figure 8b gives log $((1 - \theta_J)/\theta_J)$ *vs.* pMg. These data yield $n = 1.0$ and $pK_{app} = 3.6$ suggesting that the $\Delta F'$ phase of the fluorescence change might be due to binding a single Mg^{2+}. A comparison of the high pMg plateau level of $\Delta F'$, $\Delta F'_{max}$, with the lower titration curve in Figure 3a shows that $\Delta F'_{max}$ is of the same size as expected for deprotonation of IV at pH 6. That the rapidity of the ionization effects was presumably associated with $\Delta F'$ was confirmed by the finding that the emission changes accompanying a pH jump in the absence of Mg^{2+} are too rapid to follow by manual techniques. These facts lead to the speculation that the rapid portion of the signal change is due to a deprotonation of IV resulting from an initial Mg^{2+} association. This postulation also explains why no rapid phase is observed at pH 7.5, since at that pH all of IV is deprotonated even in the absence of Mg^{2+}.

Kinetic Mechanism and Analysis. In spite of the marked differences in the equilibrium binding curves between pH 6.0 and 7.5, the kinetic data are quite similar. In each case two slow processes are observed, although the $Mg^{2+} \rightarrow \infty$ rates at pH 6 are about a factor of 3 lower than the equivalent rates at pH 7.5. All of the λ *vs.* [Mg^{2+}] plots show hyperbolic dependence on Mg^{2+} concentration, although the midpoints of the curves at pH 6 fall at somewhat lower Mg^{2+} concentrations. The only qualitative difference in the two sets of observations is the appearance of the rapid phase ($\Delta F'$) at pH 6, and this difference is reasonably accounted for in terms of the protonation sensed by the probe. In light of these similarities, it is not unreasonable to suppose that a very similar mechanism is operating at pH 6 as at pH 7.5.

In order to extend to pH 6 the mechanism derived for pH 7.5, it is first necessary to reconsider the cause of $\Delta F'$. It has been pointed out that $\Delta F'$ is probably caused by a deprotonation step of the type

$$RH \rightleftarrows R + H^+ \qquad (2)$$

where the RH ⇄ R equilibrium refers to the ionization monitored by the probe. Since the rapid fluorescence change upon Mg^{2+} addition obviously precedes either of the unimolecular processes, it is logical to have eq 2 as the first step in the mech-

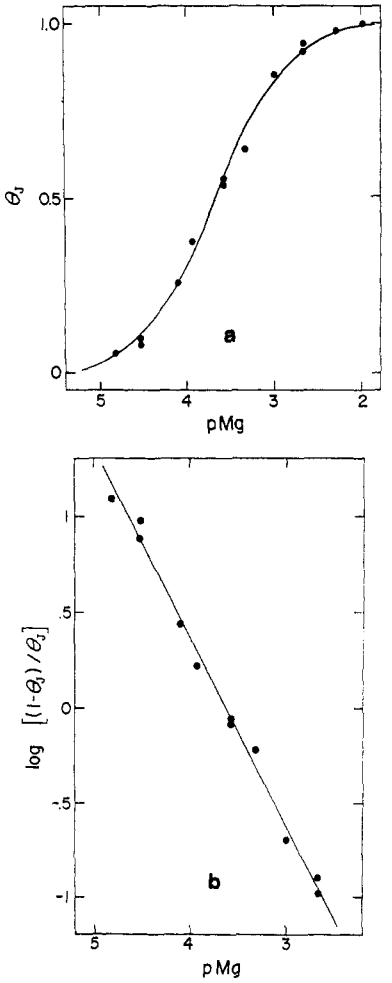

FIGURE 8: (a) Plot of θ_J *vs.* pMg, at pH 6.0, 25° with a buffer containing 10 mM Na^+, 20 mM cacodylate, 1 mM EDTA, and Cl^- counterion. See text for details. (b) Plot of log $(1 - \theta_J)/\theta_J$ *vs.* pMg. Data are derived from the curve in Figure 8a. See text for details.

TABLE III: Kinetic Parameters at pH 6.0, 25°.[a]

Rate Constant (sec^{-1})		Equilibrium Constant (M)	
k_2	0.115	K_1	1.1×10^{-4}
k_{-2}	0.005	K_3	8.0×10^{-4}
k_4	0.030	$K_H = K_0$	$10^{-6.0}$
k_{-4}	0.0005		

[a] All kinetic parameters were derived from data obtained at pH 6.0, 25° with solutions containing 1 mM EDTA, 20 mM cacodylate, 10 mM Na^+, and Cl^- counterion.

anism. This will happen if Mg^{2+} preferentially binds to R and thus promotes dissociation of HR. Therefore, the overall scheme may be written as

$$\begin{aligned} RH &\underset{k_0}{\overset{k_{-0}}{\rightleftharpoons}} R + H^+ \\ R + Mg^{2+} &\underset{k_{-1}}{\overset{k_1}{\rightleftharpoons}} X_1 \underset{k_{-2}}{\overset{k_2}{\rightleftharpoons}} X_2 \qquad (3) \\ X_2 + Mg^{2+} &\underset{k_{-3}}{\overset{k_3}{\rightleftharpoons}} X_3 \underset{k_{-4}}{\overset{k_4}{\rightleftharpoons}} X_4 \end{aligned}$$

It is again assumed that bimolecular steps in the mechanism are rapid compared to the $X_1 \rightleftarrows X_2$ and $X_3 \rightleftarrows X_4$ steps. Above *ca.* pH 7, eq 3 reduces to the mechanism studied at pH 7.5 (Lynch and Schimmel, 1974) since dissociation of RH to R is complete at that pH. Other mechanisms may be eliminated, as pointed out elsewhere (Lynch, 1973; Lynch and Schimmel, 1974).

The rate equations for the above mechanism may be derived in a manner analogous to that described in the preceding paper (Lynch and Schimmel, 1974). Some details are given in Appendix I. The solution of these equations gives expressions for λ_1 and λ_2 which may be used to extract equilibrium and kinetic parameters for the mechanism in the same manner as described in Lynch and Schimmel (1974). Results of this analysis are tabulated in Table III (where the equilibrium constant $K_i = k_{-i}/k_i$). The curves in Figures 7a and b were calculated on the basis of these parameters. It is seen that agreement of calculated with observed behavior is very good.

Two additional sets of data were tested for their compliance to the proposed mechanism. The first was the θ *vs.* pMg plot in Figure 1. Relative fluorescences were assigned to each of the species in the mechanism based on the amplitudes of three kinetic phases. An expression was derived for θ *vs.* $[Mg^{2+}]$ by using these relative fluorescence assignments together with the parameters in Table III. Appendix II gives additional details. The calculated values of the parameters characterizing the titration curve are $n = 1.32$, $pK_{app} = 4.73$; the observed values of these parameters are $n = 1.26$, $pK_{app} = 4.84$.

The second additional item of data tested against the mechanism was the amplitude $\Delta F'$ of the initial jump phase of the kinetics. According to our interpretation, this arises from deprotonation of RH caused by binding of Mg^{2+} to R. This involves the first two steps of the mechanism and the entire fluorescence change comes from the $RH \rightarrow R + X_1$ conversion since the emissions of R and X_1 are the same. We can therefore use the θ_J *vs.* pMg plot (Figures 8a and b) to calculate K_1. This calculation is given in Appendix II. The value so calculated is 1.2×10^{-4} M. The value obtained from the kinetic data (the λ_1 *vs.* $[Mg^{2+}]$ plot in Figure 7a) is 1.1×10^{-4} M (see Table III). It is clear that all available data conform extremely well to the proposed mechanism.

TABLE IV: Comparison of Equilibrium Constants at pH 7.5 and pH 6.0.

	pH 7.5 20°, 15 mM Na^+	pH 6.0 25°, 10 mM Na^+
K_{app}, M	2.3×10^{-6}	1.4×10^{-5}
n	1.8	1.3
K_1, M	4.2×10^{-4}	2.2×10^{-4} [a]
K_2	1.0×10^{-2}	4.4×10^{-2}
K_3, M	17×10^{-4}	8.0×10^{-4}
K_4	1.0×10^{-3}	17×10^{-3}
K_5, M	8×10^{-6}	
K_I, [b] M	4×10^{-6}	1×10^{-5}
K_{II}, [b] M	2×10^{-6}	1×10^{-5}

[a] $K_{1_{app}} = [Mg^{2+}]_{1/2,\lambda_1} = K_1/(1 + [H^+]/K_H)$. $[Mg^{2+}]_{1/2,\tau_1}$ is the midpoint of the τ_1 *vs.* $[Mg^{2+}]$ plot. [b] $K_I = K_1/(1 + 1/K_2)$; $K_{II} = K_3/(1 + 1/K_4)$.

It is of considerable interest to compare the numerical values of the various equilibrium constants obtained at pH 6 with those at pH 7.5. Such a comparison should permit identification of the step(s) responsible for the tenfold drop in Mg^{2+} binding affinity and the large decrease in apparent cooperativity observed at pH 6. The conditions for the two sets of kinetic experiments were slightly different: the pH 6 data were obtained at 25°, 10 mM Na^+, while data at pH 7.5 were obtained at 20°, 15 mM Na^+. The use of identical temperatures and Na^+ concentrations would further accentuate the differences between the data at pH 6 and pH 7.5, as may be seen by the greater cooperativity and Mg^{2+} affinity evident in the Mg^{2+} titration at pH 7.5, 10 mM Na^+, 25° as opposed to one at pH 7.5, 15 mM Na^+, 20° (see Lynch and Schimmel, 1974).

The comparative data are listed in Table IV; the constants K_I and K_{II} are the apparent overall binding constants for each Mg^{2+} ion in the mechanism and are defined in the table legend. All of the parameters vary somewhat between the two pH values with the Mg^{2+} association constants K_1 and K_3 being stronger at pH 6. However, each of the isomerization constants K_2 and K_4 decreases in going from pH 7.5 to pH 6, with the most outstanding change coming in the $X_3 \rightleftarrows X_4$ isomerization. The net effect of these changes is to make weaker the overall association of Mg^{2+} ions monitored by the probe.

It is also evident why the apparent cooperativity decreases at pH 6. The apparent dissociation constants change their *relative values* between pH 7.5 and pH 6; at pH 7.5, $K_{II} < K_I$ but at pH 6, $K_{II} = K_I$. The weakening of K_{II} relative to K_I has the effect of spreading the fluorescence change over a larger range of Mg^{2+} values, thereby lowering the apparent cooperativity. In addition, the Mg^{2+} induced conversion of RH to R gives a contribution to the overall fluorescence change at pH 6 which is not present at pH 7.5. This gives greater weight, at pH 6, to the fluorescence change associated with the first Mg^{2+} binding, which in turn manifests itself in a greater first power Mg^{2+} component in the log $(1 - \theta)/\theta$ *vs.* pMg plots.

Finally, the temperature dependence of k_2 and k_4 was measured at pH 6 (for procedure see Lynch, 1973; Lynch and Schimmel, 1974). Values of 30 and 39 kcal mol^{-1} were obtained for the activation energies for the $X_1 \rightarrow X_2$ and $X_3 \rightarrow X_4$ conversions, respectively. Essentially the same values for each rate constant and activation energy were obtained in both 10 mM Na^+ and 45 mM Na^+. At pH 7.5 the two activa-

tion energies are less—27 and 33 kcal mol^{-1}, respectively (Lynch and Schimmel, 1974). The tendency for the activation energies to be somewhat higher at pH 6 is consistent with the notion that the presumed aberrant structure which is formed in low salt and the absence of Mg^{2+} (Cole *et al.*, 1972; Lynch and Schimmel, 1974) is somewhat more stable at pH 6 than at pH 7.5 due to the "abnormal" protonations. Since $X_1 \rightarrow X_2$ and $X_3 \rightarrow X_4$ conversions are believed to represent the breakdown of aberrant structures on the pathway to the native form (Lynch and Schimmel, 1974), it is reasonable that activation energies for these steps should be higher at pH 6 where the aberrant forms have greater stability.

Finally, the question was also raised as to the effect of other cations in facilitating the folding of tRNA. Both Na^+ and spermidine^{3+} were tried as alternatives to Mg^{2+}. It was found that addition of these ions gave rise to rate process and activation energies similar to those observed with Mg^{2+}.

Environment of Probe. It is of interest to attempt to determine the environmental states of the probe which bring about the remarkable emission changes induced by varying pH and metal ion concentration. This is perhaps best accomplished by first comparing the emissions of the labeled tRNA and its fragments on the same absolute scale, and by fluorescence lifetime and polarization measurements on the derivatized tRNA under various conditions.

Figure 9 places the fluorescence pH titrations of intact tRNA (IV) and fragment II on the same scale. The relative positions of the curves were assigned on the basis of an experiment in which IV and II were obtained at the same concentration by directly converting IV in solution to II with RNase A. It is apparent from this figure that the conformational change induced in the tRNA by the addition of Mg^{2+} at pH 7.5 has the effect of elevating the probe's quantum yield to almost its value on II. This suggests that the conformational change induced by the addition of Mg^{2+} concludes with the 3′-terminus of the tRNA in a conformation similar to that of II, *i.e.*, exposed to the solution and not interacting with the tRNA structure to any great extent. Therefore, the probe (and the 3′-terminus) in the low salt form is probably undergoing some interaction with the tRNA which results in fluorescence quenching.

Further support for the conclusion that in the high salt, high pH form of IV the probe is freely exposed to solution comes from fluorescence lifetime and polarization data. The fluorescence lifetimes of both I and IV were measured at pH 7.5 and 10 mM Mg^{2+}. The apparent lifetimes for I and IV are 13 ± 1 and 10 ± 1 nsec, respectively. The similarity in lifetime for I and IV implies a similar quantum yield, which suggests a similar environment for each species.

The fluorescence polarizations of I, II, and the high salt, high pH form of IV are indistinguishable from background (*i.e.*, zero polarization). Since all three have similar quantum yields (and lifetimes) this implies that the probe attached to the 3′-end of IV is rotating in solution independently of the whole tRNA molecule. In contrast, IV has a polarization of *ca.* 0.06 at pH 7.5 in 15 mM Na^+, and a polarization of *ca.* 0.15 at pH 3.7 in 10 mM Na^+. However, it is difficult to measure directly the lifetimes or polarized decays of the low salt forms, because at the concentrations required for sufficient emission, scattering causes serious interference. The lifetimes of the low salt species can be estimated from the lifetime of the high salt, high pH form (10 nsec) and the relative emission intensities of the different species (see Becker, 1969). From these data, it is estimated that the rotational unit associated with the probe in the low salt forms is significantly greater

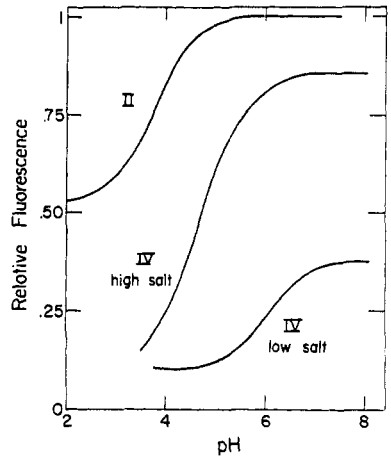

FIGURE 9: Sketch of titration curves of II and IV with and without Mg^{2+}. There is no difference in the curves for II. The curves for IV are from Figure 3a.

than the volume of the fluorphor itself (Lynch, 1973; also, unpublished calculation). Hence, the probe is at least somewhat immobilized in the low salt species. Finally, it is not possible to reach the low pH fluorescence plateau at high [Mg^{2+}] because of tRNA precipitation, and definitive polarization data on the low pH form were not obtained.

If the probe in its highly quenched state is somewhat immobilized on the tRNA, what is its environment? This question was investigated by studying the emission of I in various nonaqueous solvents. With the exception of 95% ethanol (which caused no quenching), all of the solvents used showed some quenching relative to an aqueous solution. Isopropyl alcohol, 1-butanol, dioxane, tetrahydrofuran, and ethyl ether all caused a moderate quenching of 15–30%. A chloroform–ethanol mixture (2:1 by volume) quenched two-thirds of the fluorescence, and a CCl_4–ethanol mixture (1:1 by volume) quenched 99% of the fluorescence. In all cases, the emission maximum remained substantially unchanged. Thus, it would appear that while a general quenching occurs in nonaqueous environments, the specific effects of the chlorocarbon solvents cause the more drastic quenching similar to that found in titrating tRNA from a high salt, high pH state to a low salt, low pH form. On the basis of these data, it is not possible to assign a probable location to the probe's interaction with the tRNA structure, other than to suggest that the quenching might result from a specific interaction (such as with a phosphate group) rather than a general effect caused by a nonaqueous environment.

Discussion

The data obtained by the fluorescence probe have indicated a remarkable effect, hitherto unrecognized, of pH upon the cooperative binding of Mg^{2+} to tRNA near neutral pH. Earlier studies which demonstrated cooperative Mg^{2+} binding were done above pH 7 where the pH effects are not evident (Cohn *et al.*, 1969; Danchin and Guéron, 1970; Danchin, 1972; Schreier and Schimmel, 1974). The single salt dependent pK_H detected by fluorescence ranges from $pK_H = 6$ (low salt) to $pK_H = 4.6$ (high salt). It is probably due to a cytidine residue near the probe and is doubtless typical of other "abnormal" ionizations on the tRNA. The effects of pH on the Mg^{2+} binding arise because protonation lends increased stability to the low salt, Mg^{2+}-free form of tRNA. A prime result of these protonations is to make the Mg^{2+}-induced uni-

molecular steps ($X_1 \rightarrow X_2$ and $X_3 \rightarrow X_4$, see eq 3) associated with breakdown of the low salt structure less facile at pH 6 as opposed to pH 7.5. The net effect is to reduce both the cooperativity and affinity of Mg^{2+} binding and to slow down the rate of folding of tRNA into its native structure, when Mg^{2+} is added to a low salt form.

It is of interest to draw a more concrete picture of the mode of action of the probe and its sensitivity to structural changes in the tRNA. A logical possibility is that it intercalates into the tRNA under certain conditions, since it is known that certain planar aromatic molecules have a tendency to intercalate into nucleic acid helices. The binding of proflavine to DNA has been extensively studied by Li and Crothers (1969) and the binding of ethidium to tRNA has been characterized by several workers (Bittman, 1969; Tao *et al.*, 1970; Tritton and Mohr, 1973). These molecules bind quite well to the nucleic acids (with dissociation constants of 10^{-5}–10^{-6} M), but both are positively charged, a fact which accounts for much of their binding strength. For the binding of proflavine to DNA, Li and Crothers (1969) were able to resolve a two-step mechanism in which the first step represents binding of the proflavine to the outside of the DNA helix, and the second step represents the intercalation of proflavine into the helix. For the intercalation step they found an equilibrium constant of about 10 in favor of intercalation. It can be envisioned that in low salt the probe, in the present study, is involved in an intercalation which results in fluorescence quenching and polarization. This intercalation might occur in the amino acid acceptor helix. The way in which the probe is expelled could be quite subtle. Folding of the tRNA into a tertiary structure could, for example, cause a slight change in the pitch of the acceptor helix which might in turn cause decreased intercalation of the probe. Thus, the degree of emission of transient intermediates such as X_2 could be determined by the distribution of the probe between its free and bound states. In any event, one of the reasons for the great utility of the naphthoxyl probe in this work must lie in a gentle and easily altered mode of interaction with the tRNA.

Finally, the question of the generalization of these results to other tRNAs is of interest since all results were obtained with a specific species, $tRNA^{Ile}$. To answer this question, some experiments were carried out with derivatized $tRNA^{Ala}$ (*E. coli*). Preliminary experiments showed that the emission of the probe attached to this tRNA is also sensitive to Mg^{2+} and pH in a manner analogous to that found with $tRNA^{Ile}$ (Lynch, 1973). This suggests that the results reported in this and the preceding paper (Lynch and Schimmel, 1974), could be rather general.

Appendix I

Derivation of Rate Equations for Eq 3. The rate equations for the two slow steps of eq 3 may be derived by the procedure outlined in Lynch and Schimmel (1974). It is assumed that the free Mg^{2+} concentration is constant during the kinetic events (see Lynch and Schimmel, 1974). The two rate equations are

$$-d(\Delta HR + \Delta R + \Delta X_1)/dt = k_2\Delta X_1 - k_{-2}\Delta X_2 \quad \text{(I-1)}$$

$$-d\Delta X_4/dt = -k_4\Delta X_3 + k_{-4}\Delta X_4 \quad \text{(I-2)}$$

and the conservation equation among tRNA species is

$$\Delta HR + \Delta R + \Delta X_1 + \Delta X_2 + \Delta X_3 + \Delta X_4 = 0 \quad \text{(I-3)}$$

where ΔX_i is the deviation of the concentration of X_i from its final equilibrium value. The various equilibrium constant relationships, for the steps which are rapid compared to the two slow ones, may be differentiated to give relationships among the various species. (For example, $K_H = [R][H^+]/[RH]$ and $\Delta RH = ([H^+]/K_H)\Delta R$, where it is assumed $\Delta H^+ = 0$ owing to buffering.) These relationships together with eq I-3 enable elimination of all terms except ΔX_1 and ΔX_4 from eq I-1 and I-2 with the result

$$-d\Delta X_1/dt = a_{11}\Delta X_1 + a_{12}\Delta X_4 \quad \text{(I-4a)}$$

$$-d\Delta X_4/dt = a_{21}\Delta X_1 + a_{22}\Delta X_4 \quad \text{(I-4b)}$$

where

$$a_{11} = \frac{k_2}{1 + K_1/[Mg^{2+}][1 + [H^+]/K_H]} + \frac{k_{-2}}{1 + [Mg^{2+}]/K_3} \quad \text{(I-5a)}$$

$$a_{12} = \frac{k_{-2}}{[1 + (K_1/[Mg^{2+}])(1 + [H^+]/K_H)][1 + [Mg^{2+}]/K_3]} \quad \text{(I-5b)}$$

$$a_{21} = \frac{k_4[1 + (K_1/[Mg^{2+}])(1 + [H^+]/K_H)]}{(1 + K_3/[Mg^{2+}])} \quad \text{(I-5c)}$$

$$a_{22} = \frac{k_4}{1 + K_3/[Mg^{2+}]} + k_{-4} \quad \text{(I-5d)}$$

The solution to eq I-4a,b involves finding the λ_i's of eq 1 (of the text) which are the eigenvalues of the determinant formed from the a_{ij}'s of eq I-4a,b. These are

$$\lambda_{1,2} = \frac{(a_{11} + a_{22}) \pm \sqrt{(a_{11} + a_{22})^2 + 4(a_{12}a_{21} - a_{11}a_{22})}}{2} \quad \text{(I-6)}$$

where λ_1 corresponds to the top sign and λ_2 to the bottom sign.

Rate constants may be extracted from the various limiting forms of the λ_i's as discussed in Lynch and Schimmel (1974).

Appendix II

Derivation of θ in Terms of Fluorescent Species. Relative fluorescence values may be assigned to all of the species in eq 3 by the same procedure as used in Lynch and Schimmel (1974). The values at pH 6 (10 mM Na^+) are

$$\begin{aligned} f_{HR} &= 0.33f_R \\ f_{X_1} &= f_R \\ f_{X_2} &= 1.16f_R \\ f_{X_3} &= 1.16f_R \\ f_{X_4} &= 2f_R \end{aligned} \quad \text{(II-1)}$$

The initial fluorescence F_i and final fluorescence F_f are given by

$$F_i = [HR]_i f_{HR} + [R]_i f_R \quad \text{(II-2)}$$

$$F_f = [R_0]f_{X_4} = 2[R_0]f_R \quad \text{(II-3)}$$

where $[R_0] = [RH] + [R] + [X_1] + [X_2] + [X_3] + [X_4]$. The fluorescence F at any concentration of Mg^{2+} is

$$F = [HR]f_{HR} + [R]f_R + [X_1]f_{X_1} + [X_2]f_{X_2} + [X_3]f_{X_3} + [X_4]f_{X_4} \quad \text{(II-4)}$$

Using eq II-1 and the definition of θ we obtain

$$\theta = \frac{F - F_i}{F_f - F_i} = \frac{2[X_1] + 3[X_2] + 3[X_3] + 8[X_4]}{8[R_0]} \quad \text{(II-5)}$$

where the fact that [R] = [RH] at pH 6 has been used. Dividing through by [R] gives

$$\theta = \frac{\frac{2[Mg^{2+}]}{K_1} + \frac{3[Mg^{2+}]}{K_1K_2} + \frac{3[Mg^{2+}]^2}{K_1K_2K_3} + \frac{8[Mg^{2+}]^2}{K_1K_2K_3K_4}}{8\left(2 + \frac{[Mg^{2+}]}{K_1} + \frac{[Mg^{2+}]}{K_1K_2} + \frac{[Mg^{2+}]^2}{K_1K_2K_3} + \frac{[Mg^{2+}]^2}{K_1K_2K_3K_4}\right)} \quad \text{(II-6)}$$

A log $((1 - \theta)/\theta)$ *vs.* pMg line may be generated with eq II-6, by using the values of K_1, K_2, K_3, and K_4 obtained from the kinetic curves. The line so generated is linear over the range of $0.05 < \theta < 0.95$. The n and pK_{app} values obtained are 1.32 and 4.73, respectively, which agrees well with the observed values of 1.26 and 4.84, respectively. Although additional binding beyond the X_4 stage could be taken into account, the calculated behavior agrees satisfactorily enough without considering it.

The amplitude of the rapid jump in fluorescence, $\Delta F'$, shows a sigmoidal dependence on pMg. It is possible to derive an expression for the fractional values of this fluorescence jump, $\theta_J = \Delta F'/\Delta F'_{max}$. This may be done by considering the steps

$$\begin{aligned} RH &\overset{K_H}{\rightleftharpoons} R + H^+ \\ R + Mg^{2+} &\overset{K_1}{\rightleftharpoons} X_1 \end{aligned} \quad \text{(II-7)}$$

Using the partial fluorescence of eq II-1 and the equality of [R] and [RH] at pH 6, we obtain

$$\begin{aligned} F_i &= f_{HR}[HR]_i + f_R[R]_i = 2f_{HR}[R'_0] \\ F_f &= f_{X_1}[X_1]_f = 3f_{HR}[R'_0] \end{aligned} \quad \text{(II-8)}$$

$$F = f_{HR}[HR] + f_R[R] + f_{X_1}[X_1] = 4f_{HR}[HR] + 3f_{HR}[X_1]$$

where $[R'_0] = [RH] + [R] + [X_1]$. The expression for θ_J is

$$\theta_J = \frac{F - F_i}{F_f - F_f} = \frac{[X_1]}{[RH] + [R] + [X_1]} \quad \text{(II-9)}$$

or

$$\theta_J = \frac{1}{(K_1/[Mg^{2+}])\,[1 + ([H^+]/K_H)] + 1} \quad \text{(II-10)}$$

where $K_H = 10^{-6} = [H^+]$ at pH 6. It is clear from eq II-10 that it is possible to obtain K_1 directly from the observed midpoint of the $\Delta F'$ *vs.* $[Mg^{2+}]$ curve. See text for further discussion.

References

Alberty, R. A., Smith, R. M., and Bock, R. M. (1951), *J. Biol. Chem. 193*, 425.

Azumi, T., and McGlynn, S. P. (1962), *J. Chem. Phys. 37*, 2413.

Becker, R. S. (1969), Theory and Interpretation of Fluorescence and Phosphorescence, New York, N. Y., Wiley.

Beers, R. F., Jr., and Steiner, R. F. (1957), *Nature (London) 179*, 1076.

Bittman, R. (1969), *J. Mol. Biol. 46*, 251.

Cavalieri, L. F., and Stone, A. L. (1955), *J. Amer. Chem. Soc. 77*, 6499.

Chen, R. F., and Bowman, R. L. (1965), *Science 147*, 729.

Cohn, M., Danchin, A., and Grunberg-Manago, M. (1969), *J. Mol. Biol. 39*, 199.

Cole, P. E., Yang, S. K., and Crothers, D. M. (1972), *Biochemistry 11*, 4358.

Cox, R. A., and Peacocke, A. R. (1957), *J. Chem. Soc.*, 4724.

Danchin, A. (1972), *Biopolymers 11*, 1317.

Danchin, A., and Guéron, M. (1970), *Eur. J. Biochem. 16*, 532.

Eigen, M., and Hammes, G. G. (1960), *J. Amer. Chem. Soc. 82*, 5951.

Hartman, K. A., Jr., and Rich, A. (1965), *J. Amer. Chem. Soc. 87*, 2033.

Hayes, N. V., and Branch, G. E. K. (1943), *J. Amer. Chem. Soc. 65*, 1555.

Jordan, D. O. (1960), The Chemistry of the Nucleic Acids, Washington, D. C., Butterworths.

Jordan, D. O., Mathieson, A. R., and Matty, S. (1956), *J. Chem. Soc.*, 158.

Laitinen, H. A. (1960), Chemical Analysis, New York, N. Y., McGraw-Hill.

Langridge, R., and Rich, A. (1963), *Nature (London) 198*, 725.

Li, H. J., and Crothers, D. M. (1969), *J. Mol. Biol. 39*, 461.

Lynch, D. C. (1973), Ph.D. Thesis, M.I.T.

Lynch, D. C., and Schimmel, P. R. (1974), *Biochemistry 13*, 1841.

Rich, A., Davies, D. R., Crick, F. H. C., and Watson, J. D. (1961), *J. Mol. Biol. 3*, 71.

Saneyoshi, M., Harada, F., and Nishimura, S. (1969), *Biochim. Biophys. Acta 190*, 264.

Schreier, A. A., and Schimmel, P. R. (1974), *J. Mol. Biol.* (in press).

Steiner, R. F., and Beers, R. F., Jr. (1959), *Biochim. Biophys. Acta 33*, 470.

Tao, T., Nelson, J. H., and Cantor, C. R. (1970), *Biochemistry 9*, 3514.

Tritton, T. R., and Mohr, S. C. (1973), *Biochemistry 12*, 905.

Yarus, M., and Barrell, B. G. (1971), *Biochem. Biophys. Res. Commun. 43*, 729.